JOURNAL OF MATERIALS SCIENCE 19 (1984) 3477–3486

The hydration of tricalcium silicate in the presence of colloidal silica

ZHAO-QI WU*, J. F. YOUNG
Departments of Civil Engineering and Ceramic Engineering, University of Illinois, Urbana, Illinois 61801, USA

Reactions of colloidal silica fumes with calcium hydroxide or hydrating tricalcium silicate (C_3S) have been studied using calorimetry, chemical analyses, and scanning electron microscopy. Silica fume reacts immediately with calcium hydroxide forming a colloidal calcium silicate hydrate (C–S–H) similar to that formed by the hydration of C_3S. When excess silica is present it reacts with C–S–H already formed to produce a new, highly polymerized C–S–H, having a very low C/S ratio (1.0). Silica fume accelerates the hydration of C_3S, reduces the amount of calcium hydroxide formed by reacting with it, and slightly lowers the C–S–H ratio of the C–S–H formed by hydration. When large amounts of silica fume are present the formation of calcium hydroxide may be entirely suppressed and a highly polymerized C–S–H is formed. Silica fume is considered a good model for reactive pozzolans used in concrete.

1. Introduction

Synthetic colloidal silica formed by vapour phase hydrolysis of silicon compounds (silica fume) is a highly reactive siliceous material. As such it would be expected to act as a very reactive pozzolan† in Portland cement paste. An earlier study [1] has confirmed this. In addition it has been shown [1–3] that the presence of small amounts of silica fume can accelerate the hydration of tricalcium silicate (C_3S‡), the principal constituent of Portland cement, thereby increasing the rate of early strength gain. In recent years silica fume became economically available as an industrial by-product and much research has been done on its use as a pozzolan for concrete [4–7]. Silica fume reacts rapidly with calcium hydroxide (CH‡) [3, 8] to form colloidal calcium silicate hydrate (C–S–H‡) and capillary porosity is reduced substantially [8]. Cement pastes or concretes made with silica fume thus exhibit very high early and ultimate strength, and excellent durability. Silica fume has also been used to develop very low porosity cement-composites [7, 9] that have strength and durability comparable to ceramic materials.

There are still many questions needed to be clarified concerning the chemical interactions between cement and silica, which is an intrinsically interesting system involving colloidal reactants and colloidal products. Although high pozzolanic activity of silica fume is commonly observed, Chatterji *et al.* [10] claimed that silica fume has little activity. It is not yet clear whether the more rapid hydration of C_3S in the presence of silica fume is due to its very small particle size, or to its chemical reactivity. The reaction product of lime and silica fume appears to be C–S–H(I) [11], but the C/S ratio was reported to be 1.1 [4] and 1.3 [8]; the possibility that silica fume can react with C–S–H formed from C_3S hydration also exists.

The purpose of this work is to understand better the effect of silica fume on C_3S hydration by investigating the rate of hydration, the ion concentration in the liquid phase, the composition of hydration products, and the degree of polymeri-

*Permanent address: The Research Institute of Building Materials, East suburb, Beijing, China.
†A pozzolan is a siliceous material containing amorphous or glassy silica, which reacts with the calcium hydroxide formed in hydrated cement paste.
‡Cement chemists' notation.

0022–2461/84 $03.00 + .12 © *1984 Chapman and Hall Ltd.*

TABLE I Details of silica fumes used

Designation	Description	Surface area (m^2/g)	Silica content (%)	Source
W1	Cab-o-Sil,* EH-100	200	> 99	Cabot Corp., Tuscola, IL
W2	Cab-o-Sil* L-90	90	> 99	Cabot Corp., Tuscola, IL
B	Microsilica†	20	> 95	Elborg Corp., Pittsburgh, PA

*Formed from vapour phase hydrolysis of $SiCl_4$.
†By-product in silicon production from reduction of quartz.

zation of C–S–H. Mixtures of calcium hydroxide and silica fumes were also studied in order to further elucidate the reactivity of silica fume and the nature of its reaction products. Two synthetic silica fumes were compared with one by-product silica fume.

2. Materials and methods

2.1. Materials

The C_3S[§] was obtained from the Portland Cement Association [2] and ground to a fineness of 3900 $cm^2\ g^{-1}$ (Blaine). The details of the silicas used are given in Table I. Calcium hydroxide was made by calcining reagent grade $CaCO_3$ at 1000° C, adding it to enough decarbonated, deionized water to make a slurry and then drying the slurry *in vacuo* at 60° C. Thermal analysis showed only very small amounts of calcium carbonate were present.

The samples used in this study are listed in Table II. Deionized water was used as mixing water, and the samples cured at 22° C. After one day cured in moist air, pastes of A-S0, A-S6, A-S16 and A-S52 were demoulded and stored in water; the others were kept at 100% r.h.

TABLE II Details of samples used in study

Designations[a]	C_3S	Silica	CH	C/S	W/S[b]
2CS-W1	–	29	71	2.00	1.90
CS-W1	–	45	55	1.00	1.90
2CS-W2	–	29	71	2.00	1.10
CS-W2	–	45	55	1.00	1.10
2CS-B	–	29	71	2.00	0.75
CS-B	–	45	55	1.00	0.75
A-S0	100	–	–	3.00	0.70
A-S6	94	6	–	2.44	0.70
A-S16	86	14	–	1.87	1.00
A-26	79	21	–	1.51	–
A-39	72	28	–	1.18	–
A-S52	66	34	–	1.00	1.40

[a]Denotes C/S ratio and type of silica used. The A-S series contains Cab-o-Sil EH-100.
[b]For paste samples only.

2.2. Experimental methods

The early hydration of alite with or without silica fume was monitored by calorimetry using a semi-isothermal calorimeter [12] with a sensitivity of 15 mV° C^{-1}; the sample size was 500 mg and the water: solid (w/s) ratio was 3.0, unless stated. Solutions from filtered alite suspensions (w/s = 10), were analysed for [OH^-]. The suspensions were agitated by rotation at 6 r.p.m., filtered using a millipore filter (1.2 μm); a 2 ml aliquot of the filtrate was then added to 4 ml of 0.050 N HCl and the excess acid back-titrated using 0.056 N NaOH solution.

Residual unreacted silica in pastes was determined using the method of Mohan and Taylor [13], except that the solid residue was retained on a quantitative filter paper, and ignited at 1000° C. Calcium hydroxide and calcium carbonate contents were measured quantitatively by thermally evolved gas analysis (TEGA), using helium as the carrier gas. (Operating conditions: heating rate, 10° C min^{-1}; flow rate, 55 ml min^{-1}; recorder sensitivity, 1 mV per 25.4 mm.) Calibration curves were established using reagent grade materials. TEGA was also used to qualitatively monitor the formation of C–S–H. Trimethylsilyl (TMS) derivatives of C–S–H were prepared according to the method of Tamas *et al.* [14] and the derivatized silicate anion species were separated and quantitatively determined by GPC, using procedures described elsewhere [15]. The microstructure and morphology of hydration products were studied

§Composition in wt%: CaO = 71.08, SiO_2 = 25.79, Al_2O_3 = 1.24, Fe_2O_3 = 0.08, MgO = 1.27, Na_2O = 0.01, K_2O = 0.00, insoluble residue = 0.20.

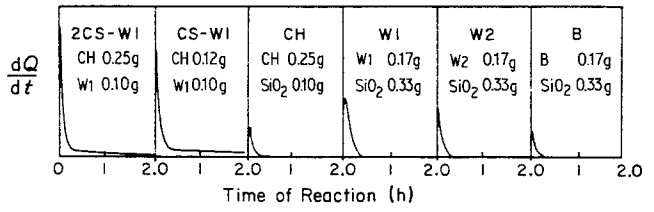

Figure 1 Rate of heat evolution of silica fumes, CH, and mixtures of the two, after initial mixing with water.

using a scanning electron microscope (SEM) (Model Jeolco JSM-U3) equipped with a non-dispersive X-ray detector (Ortec) and a multi-channel analyser (Tracor Northern, Model TM-7200).

3. Results

3.1. Mixtures of calcium hydroxide and silica fume

Fig. 1 shows the early heat evolution of CS-W1 and 2CS-W1, as well as the corresponding curves for calcium hydroxide and silica fumes. It can be seen that the first heat peak of both mixtures is higher than the combined heat of dissolution of pure CH and heat of wetting of silica fume, indicating that there is an immediate reaction between CH and silica fume upon contact with water. No second peak was observed in the first 24 h. Table III compares the reactivities of the silica fumes in terms of the consumption of calcium hydroxide and silica fume. They correlate well with surface area: the calcium hydroxide was fully consumed by the finest silica fume (W1) within 1 day, but took more than 28 days when silica fume B was used.

The X-ray diffraction patterns for CS-W1 and 2CS-W1 after reaction for 1 day are quite similar to those reported by Buck and Burkes [11]. Although the 1.25 nm peak was not observed, it is not always present [11]. The distribution of silicate ions in the reaction products is given in Table IV. In 2CS-W1 pastes the content of dimer remained almost constant, even though the CH content changed significantly in the first 24 h. In CS-W1 pastes the content of dimer began decreasing to a low level after 12 h of hydration, when the CH content had dropped to near zero. Fig. 2 shows the microstructural development of the hydrating mixtures in series of SEM micrographs. The very fine structure of silica fume (Fig. 2a) is gradually replaced by an agglomeration of larger, but still small particles (Fig. 2b). Eventually very smooth fracture surfaces are observed (Fig. 2c).

3.2. Alite–silica systems

The calorimetric curves of the A-S series are shown in Fig. 3. As the amount of silica (W1) added increases a small shoulder appears on the early heat peak, which has also been observed by Kurdowski and Nocum-Wezelik [3]. In contrast to their results, however, we always observed the second main heat peak (not shown), even when

TABLE III Analyses of lime–silica mixtures during the reaction period

Time	B		W2		W1					
	CS-B CH	2CS-B CH	CS-W2 CH	2CS-W2 CH	CS-W1			2CS-W1		
					CH	SiO_2[a]	C/S[b]	CH	SiO_2[a]	C/S[b]
0	55.0	71.0	55.0	71.0	55.0	45.0		71.0	29.0	
1 h			50.9	70.5	27.3	27.2	1.26	56.1	20.0	1.34
3 h					23.5			53.6		
5 h	53.9	69.2	42.6	61.1	20.0	20.3	1.15	44.7	13.2	1.35
12 h			30.7	56.4	4.1	15.0	1.38	34.2	7.1	1.36
1 d	50.0	67.3	20.9	45.2	1.4			23.3	1.7	1.41
3 d	40.2	60.5	5.4	30.7	0			20.3	0	1.41
7 d	27.7	48.6	0	19.7	0	9.5	1.26	20.4	0	1.41
14 d	12.3	34.7	0	17.7		8.6	1.23			
21 d	8.2	30.6								
31 d	3.5	26.3				4.4[c]	1.10[c]			

[a]Residual unreacted silica fume.
[b]C/S ratio of C–S–H formed.
[c]Cured for 70 days.

TABLE IV Distributions of silicate species in hydrating CS-W1 and 2CS-W1 (wt% of silica in C–S–H)

Time	CS-W1							2CS-W1						
	Mono-[a]	Di-	Penta-	Octa-	C[b]	D+E[c]	Poly[d]	Mono-	Di-	Penta-	Octa-	C	D+E	Poly
5 h	7.5	50.9	23.6	9.0	6.3	2.6	41.6	10.4	67.7	17.8	4.0	0.1	0	20.8
12 h	3.7	50.2	23.4	10.9	8.2	3.6	46.1							
1 d								11.0	67.9	16.0	3.8	1.3	0	21.1
3 d	2.7	32.8	19.0	12.8	15.9	16.8	64.5	4.3	65.0	18.8	6.8	3.5	0.6	30.7
14 d	2.3	32.0	18.9	11.6	15.6	19.9	65.7	3.6	69.9	17.5	5.4	3.1	0.5	26.6
92 d	1.5	21.2	17.9	11.5	16.9	31.1	77.3	2.6	68.9	17.8	6.0	3.8	0.8	28.4

[a]Mono- = monosilicate, Di- = disilicate, etc.
[b]Silicate species with the average number of Si atoms of 14 [16].
[c]Silicate species with the average number of Si atoms of 22 or more [16].
[d]Total polysilicate, being the sum of penta- through E.

the shoulder occurred. The peak area measured over the first hour is about five times greater in A-S52 compared to that of A-S0. This indicates that early reaction was accelerated strongly by silica fume W1 and that the shoulder may represent rapid reaction between the silica fume and the CH released from the alite, as seen in Fig. 1. The change of $[OH^-]$ in the aqueous phase as a function of time (shown in Fig. 4) confirms this supposition, an early decrease in $[OH^-]$ being observed. Also TEGA analysis shows that more C–S–H is formed in the first hour of hydration as the amount of silica fume is increased. Fumes W2 and B are less reactive than W1, but if the heat peak area is plotted against total surface area of silica fume introduced in the system (as shown in Fig. 5) the relationship is linear regardless of the differences in purity and particle size. Thus the initial reactions depend only on the surface area of the silica in the system. An initial period of rapid dissolution of C_3S (the pre-induction period), which is observed by both calorimetry (Fig. 3) and $[OH^-]$ analyses (Fig. 4), precedes the induction period, a period of lower reactivity. The latter is a well-known characteristic of C_3S hydration and its end corresponds to $[OH^-]_{max}$ [16] and an increase in the rate

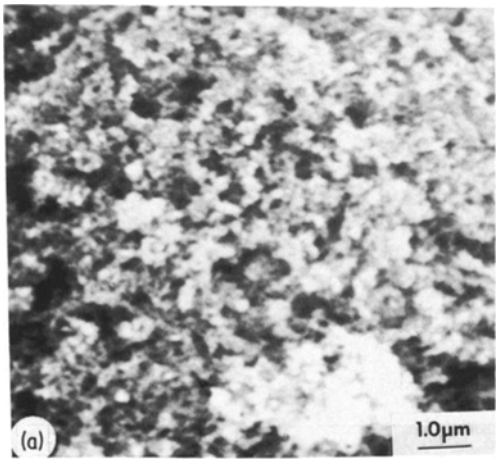

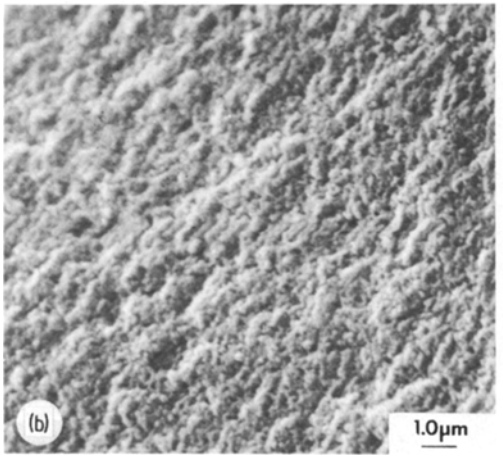

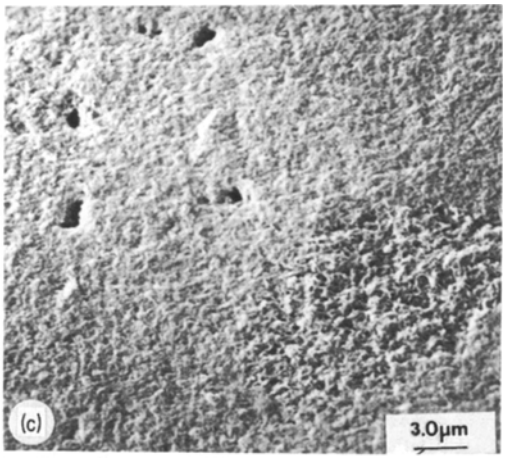

Figure 2 SEM micrographs of (a) silica fume, W1, (b) after reaction with CH for 12 h (C1-W1), and (c) after reaction with CH for 3 days (C1-W1).

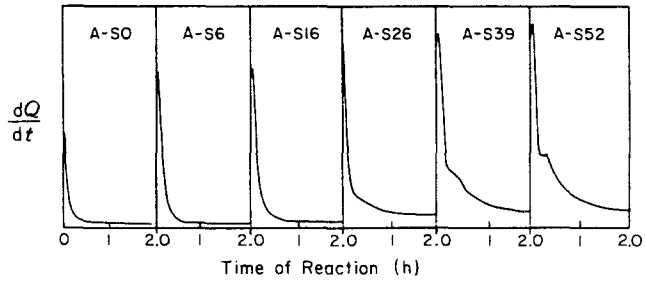

Figure 3 Rate of heat evolution of C_3S-silica fume mixtures containing varying amounts of silica fume, W1.

of heat evolution. The presence of silica fume lengthens the pre-induction period, but shortens the induction period so that the renewed hydration of C_3S starts earlier.

Degrees of hydration of C_3S (see Table V), determined by the TMS method [17] confirms this accelerating effect, which has also been observed by others [1–3, 8]. The aqueous phase always becomes supersaturated with respect to CH, even in the presence of silica fume, in contrast to earlier findings [3].

The changes of CH content with time in A-S6, A-S16, and A-S52 are shown in Table V. In system A-S52, there is almost no CH detected throughout the whole experimental period, whereas in system A-S6, the content of CH increases steadily. The smaller amount of silica apparently does not change the general course of alite hydration. It is interesting to note that there is a maximum of CH content in system A-S16 similar to that observed by Sellevold *et al.* [8], who studied cement hydrated with a silica fume similar to B. Thus the initial rate of crystallization of CH is greater than its rate of reaction with silica. Fig. 6 shows that the polysilicate content of the C–S–H formed is little affected by the presence of silica fume up to 16 wt%. In system A-S52, however, the amount of polysilicate increases rapidly after 12 h to about 80%.

Fig. 7 displays the microstructural development in C_3S paste containing silica and is representative of all systems studied, although adding more silica speeds up the rate of change. Fig. 7a shows a large C_3S grain surrounded by silica fume particles, which have already reacted, particularly those particles nearest the C_3S grains. The surface of the C_3S grain is also slightly hydrated. This is typical of the microstructure in the first few hours of hydration (e.g. 4 h A-S16, 1 h A-S52); later (Fig. 7b) reactions of both silica and C_3S are much more noticeable. Partially hydrated C_3S particles are embedded in the C–S–H formed in part by reaction with silica, and CH crystals are also visible (in A-S52 crystalline CH was never observed). As the hydration continues (Fig. 7c) the structure gets denser, but C_3S grains are still observed and some appear to pull away from the C–S–H matrix during fracturing (Fig. 7d). The C–S–H adhering to the C_3S grain particle may have a difference in morphology, at least temporarily. The matrix

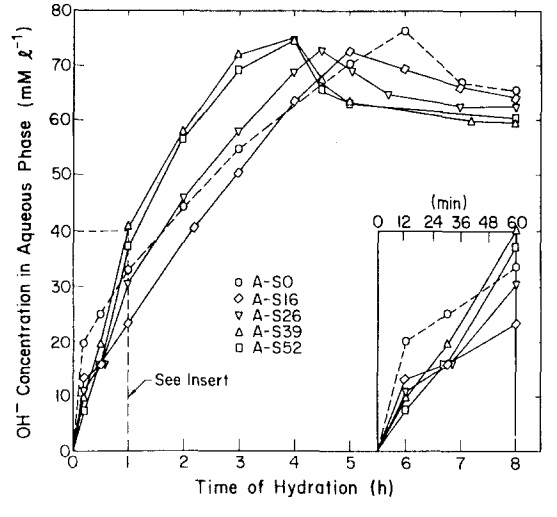

Figure 4 Release of OH^- from C_3S during the first few hours of hydration with and without silica fume.

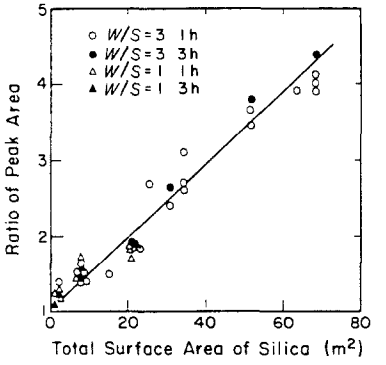

Figure 5 Area of the initial evolution peak (see Fig. 3) plotted as a function of the total surface area of added silica fume.

TABLE V Analyses of alite-silica fume mixtures during the reaction period

Time	A-S0			A-S6				A-S16				AS-52			
	α	CH	C/S	α	CH	SiO_2[a]	C/S[b]	α	CH	SiO_2[a]	C/S	α	CH	SiO_2[a]	C/S
0	0	0		0	0	6		0	0	16		0	0	52	
1 h												16.0	1.0	48.4	1.46
2 h												31.9	2.3	(45.5)[b]	1.56
4 h												(40.0)[b]	(2.0)[b]	43.5	1.53
6 h								23.7	4.3	13.8	1.76				
8 h												57.0	1.8	37.0	1.33
14 h				30.5	12.6	(5.5)[b]	1.56	47.4	14.1	(12.5)[b]	1.57				
1 d	19.6	9.7	1.47	43.6	14.9	(3.5)[b]	1.54	52.8	16.5	(11.5)[b]	1.48	65.4	3.2	(29.5)	1.20
3 d	36.6	11.8	2.01	57.4	16.8	(1.0)[b]	1.52	64.6	9.0	5.0	1.52	72.3	1.7	23.2	1.16
7 d	44.7	13.3	2.08	65.1	19.8	0	1.47	74.9	8.7	0.6	1.44	81.6	2.0	20.8	1.16
14 d	50.4	17.5	1.93	71.1	21.3	0	1.52	79.9	8.7	0	1.47	84.4	2.6	(17.0)[b]	1.12
21 d	56.8	(22.9)[b]	1.76	72.7	22.4	0	1.50								
28 d	64.6	27.2	1.64	77.4	24.2	0	1.52	85.0	10.0	0	1.49	88.9			
30 d												89.8	1.8	(13.8)[b]	1.12
37 d	91.2[c]	42.6	1.56					88.0	10.9	0	1.51	97.0[d]	0	9.7	1.11

[a]Residual unreacted silica fume.
[b]Overall C/S ratio of C–S–H formed (no distinction is made between different kinds of C–S–H – see text).
[c]Cured for 241 days.
[d]Cured for 50 days.

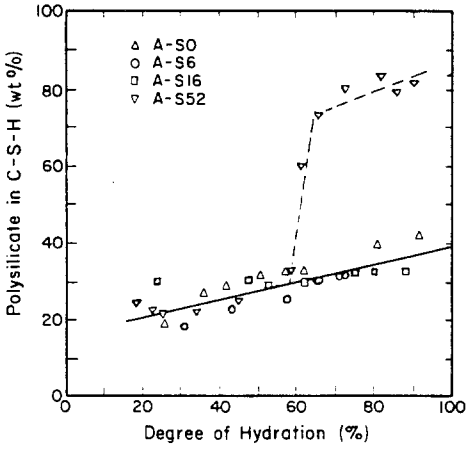

Figure 6 Amount of polysilicate in C–S–H formed in C_3S paste with and without silica fume. (The remainder is dimeric silicate.)

resembles that formed in the lime–silica mixes and shrinks markedly under the high vacuum and heating of the electron beam. Extensive cracking gradually occurred and could be observed in progress; one such crack can be seen in Fig. 7c.

4. Discussion

4.1. The effect of silica fume on the early hydration of C_3S

From Fig. 4 it was seen that the pre-induction period of C_3S hydration is lengthened and the induction period shortened by the addition of silica fume. Calorimetry, TEGA, and $[OH^-]$ plots indicated that rapid precipitation of C–S–H occurs initially. Considering the high surface are of W1, the average particle size is calculated to be around 0.01 μm, which is about 10^3 times smaller than the average size of alite grains. If 10% W1 is added, each C_3S grain will be surrounded by 10^8 silica particles, which can be considered as a silica layer enveloping each C_3S grain. Upon contact with water, the Ca^{2+} and OH^- ions released by hydrating C_3S have to pass through the layer of reactive silica to enter the bulk solution. Both Ca^{2+} and OH^- react with the silica to form C–S–H and delay the increase of Ca^{2+} and OH^- in the bulk solution. It was also observed that the *w/s* ratio strongly affects the rate of reaction between calcium hydroxide, (or C_3S) and silica fume W1. For example, with 2CS-W1 after 8 h reaction more than 30% calcium hydroxide had been consumed when $w/s = 1.4$, but only 20% when $w/s = 10$. In A-S52 pastes ($w/s = 1.4$) little or no free CH was detected using TEGA, whereas A-S52 suspension ($w/s = 10$) CH could be detected. The effect of *w/s* ratio implies that the diffusion of Ca^{2+} onto the silica surface may be the rate-controlling step. With higher *w/s* ratios the ions will encounter a smaller number of silica particles in the vinicity of the C_3S surface.

There is another factor that has also to be considered. Since W1 has high surface area (about the same order as C–S–H itself), initial C–S–H formation will most likely be at the silica surface rather than on the C_3S surface, which will remain relatively clean until all silica particles in its vicinity have reacted. The initial rapid dissolution of C_3S will thus last longer as the ions released react with silica. This explains the changes in the calorimetry curves, and was confirmed by SEM observations. From Fig. 4 it can be seen that in systems A-S39 and S-S52 the $[OH^-]$ concentration already reaches a high level at the end of the pre-induction period, and thus the induction period is shortened since $[OH^-]_{max}$ is reached sooner. After the end of the induction period precipitation of C–S–H at the C_3S surface occurs normally.

4.2. The effect of silica fume on C–S–H composition

4.2.1. Silicate polymerization

In the A-S series the distribution of silicate species in the paste is quite similar to that reported earlier [15] and is roughly independent of the silica fume content as long as appreciable quantities of CH are present. Assuming that all monomeric silicate is associated with unreacted C_3S [17], the distribution of dimeric silicate and polysilicate in C–S–H can be calculated and is plotted in Fig. 6. The polysilicate content gradually rises to about 40 wt% and is composed of primarily pentameric and octameric species. The trend is very similar in the lime–silica mixtures when unreacted CH is still present. In 2CS-W1, the polysilicate content rises to about 30%, while in CS-W1 it reaches about 46% at 12 h. In these samples the distribution of polysilicate (see Table IV) is similar to that of the A-S series. However, appreciable quantities of monomeric silicate are found in the C–S–H produced from lime–silica mixtures which suggest that the reaction of the highly polymerized silica fume is initiated by hydrolysis to the monomer followed by subsequent polymerization. At greater ages the monomer has been completely consumed, the small residuals being attributed to side reactions during derivitization.

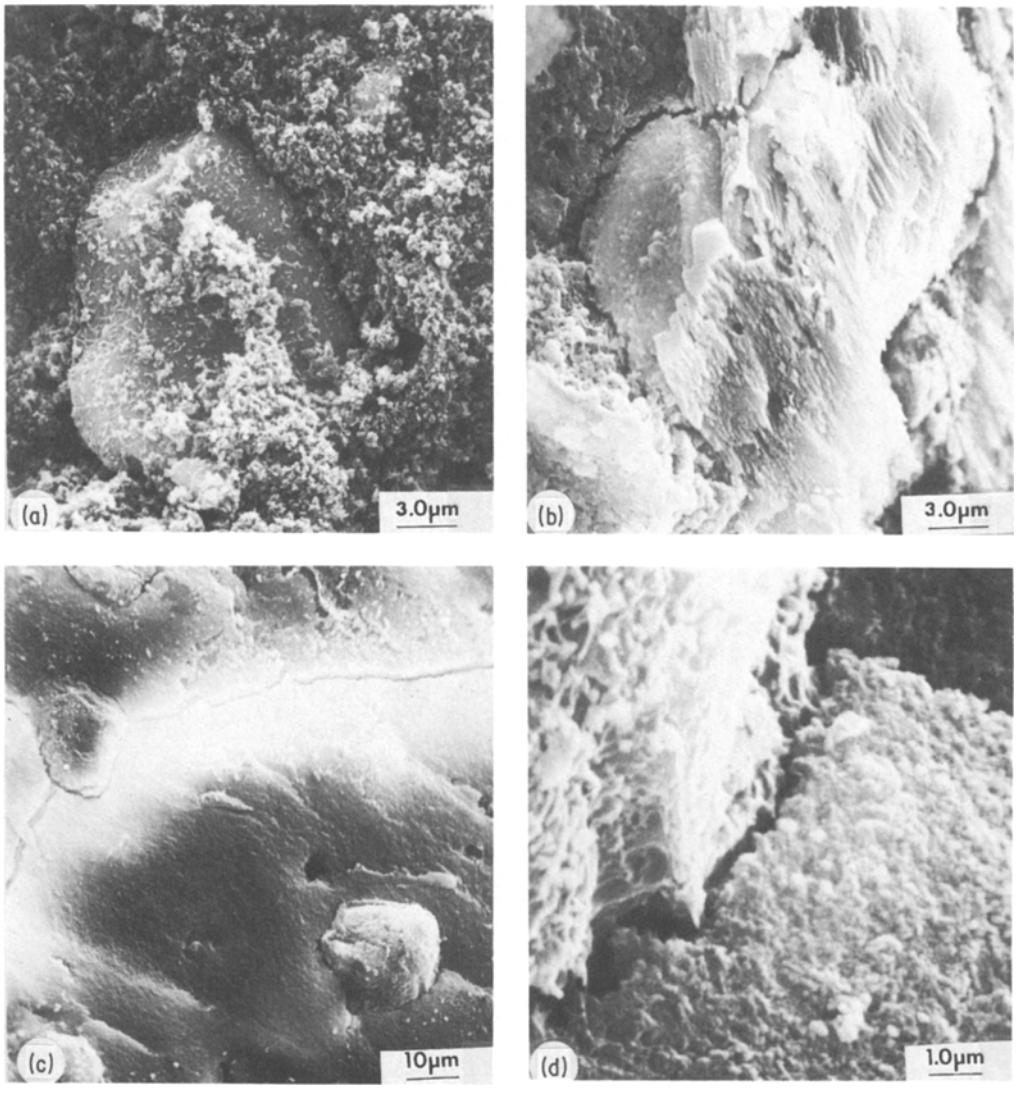

Figure 7 SEM micrographs of a C_3S paste containing silica fume (a) A-S16, 4 h, (b) A-S16, 8 h, (c) A-S52, 1 day, and (d) magnification of lower left-hand corner of (c).

When CH is completely consumed in A-S52 and CS-W1 a pronounced increase in the amount of polysilicate is observed (Fig. 6 and Table IV). Furthermore, the distribution of a silicate species within the polysilicate fraction is significantly shifted towards the high molecular weight species (see Table IV for CS-W1), mainly at the expense of the dimer. We conclude from this that silica fume probreacts preferentially with CH, either added or formed from C_3S hydration, but that it subsequently reacts with the C–S–H already formed.

4.2.2. C/S ratios

The composition of C–S–H is expression in terms of CaO/SiO_2(C/S) molar ratio. This is calculated by subtracting the CaO and SiO_2 associated with the unreacted starting materials, and CH formed during C_3S hydration, from the total CaO and SiO_2 in the systems, and assigning the differences to the C–S–H phase. These values may have rather high errors since several different analyses are involved. The C/S ratios represent an average for the total C–S–H formed; C/S ratios for the different C–S–H types postulated were not calculated because of uncertain assumptions. The values are given in Tables III and V, where it can be seen that in the A-S series the C/S ratios become somewhat lower as more silica fume was added

even though the distribution of silicate species is not very different. The calculated values for pure C_3S show similar trends to previous studies [4, 8]. The C/S ratio for C–S–H formed in the lime–silica mixtures is somewhat lower than that formed in the C_3S pastes. It would seem that the C–S–H formed from the reaction between lime and silica fume has a slightly different composition from that of C–S–H formed directly from C_3S. Semi-quantitative analyses made by SEM–EDS point scans support this view. Our results show no clear correlation between C/S ratio and silicate structure, although there is a general tendency for highly polymerized pastes to have lower C/S ratios. In samples of A-S52 and CS-W1, where the CH is all consumed, a highly polymerized C–S–H is formed and the C/S ratio had dropped to the vicinity of 1.0. The results suggest that the excess silica fume reacts with C–S–H already formed.

4.3. Silica fume as a model pozzolan

Silica fume similar to Sample B has been used as a pozzolan in Portland cement concrete for many years, particularly in Norway [4–7]. The high reactivity and high purity of synthetic silica fume makes it of interest as a "model pozzolan" to probe the nature of the pozzolanic reaction. It has been shown (see Fig. 4) that both synthetic and by-product fumes behave similarly, differing only in kinetics of reaction according to their surface areas, so that it is of interest to compare them with other pozzolans, particularly fly ash which consists of relatively coarse spheres of glassy silica. From the comparisons outlined below it is concluded that silica fume can be used to model reactive fly ashes, and reactive pozzolans in general.

The silica fume accelerates early C_3S hydration, probably by early precipitation of C–S–H at the surfaces of the silica particles. Unless there is a large excess of highly reactive silica, CH crystals will nucleate and grow, but the rate of CH formation will be less since concurrent pozzolanic consumption is occurring. The CH content may even pass through a maximum as the rate of pozzolanic reaction exceeds the rate of crystal growth. The acceleration of C_3S hydration by fly ash has been well documented [13, 18, 19] but others [19, 20] have reported retardation. It is clear [21] that fly ashes have different reactivities; so that reactive pozzolans may accelerate C_3S hydration, while less reactive ones do not [20]. Reactive pozzolans affect the aqueous phase composition [19] in a similar manner to that reported here, and there are indications [18, 19] of early precipitation of hydration products on fly ash surfaces. Reduction of the amount of CH formed in the presence of fly ash is seen at early times [13, 20], and with some pozzolans a maximum is observed [20].

From the above results and discussion it is postulated that up to three kinds of C–S–H are formed: that directly from C_3S; that formed from the reaction between CH and silica fume, which will have a slightly lower C/S ratio; and that formed from the reaction between silica fume and C–S–H, which produces a highly polymerized C–S–H with a very low C/S ratio. The C–S–H from C_3S will be found predominantly in the regions formerly occupied by unhydrated grains, while the other kinds of C–S–H will be found in the intergranular regions and probably intimately mixed. However the highly polymerized C–S–H will only form if there is excess silica over the amount required to consume all CH. Thus the mean C/S ratio of the C–S–H will be somewhat lower than normal away from the C_3S grains, but the distribution of silicate polymers in C–S–H will not be very different, at least initially. The C/S ratio of the C–S–H matrix is lower [13, 20, 22] and a zonal structure for C–S–H has been reported [20], although this claim requires further confirmation. The silicate structure of C–S–H is initially not much changed by the presence of fly ash [13]. It is thus concluded that silica fume can be used to model a reactive fly ash and perhaps reactive pozzolans in general.

5. Conclusions

1. Silica fume accelerates early hydration of C_3S by providing large amounts of reactive siliceous surface, which serves as a site for early C–S–H precipitation. The reactivity of silica fume mainly depends on its specific surface area.

2. The reaction between calcium hydroxide and silica fume begins immediately. The reaction product is similar to the C–S–H formed in C_3S hydration, but the C/S ratio is slightly lower. However, unless large amounts of silica fume are present the rate of formation of CH from hydrating C_3S is greater than its rate of consumption by reaction with silica fume.

3. When all calcium hydroxide is consumed the excess silica can react with C–S–H already formed

to produce another kind of C–S–H, with a low C/S ratio, which is highly polymerized.

4. Silica fume can be used to model the interaction of fly ash, or other reactive pozzolans, with C_3S in Portland cement.

References

1. J. A. NELSON and J. F. YOUNG, *Cem. Concr. Res.* **7** (1977) 227.
2. H. N. STEIN and J. M. STEVELS, *J. Appl. Chem.* **14** (1964) 338.
3. W. KURDOWSKI and W. NOCUM-WEZELIK, *Cem. Concr. Res.* **13** (1983) 341.
4. A. TRAETTEGERG, *Cemento* **75** (1978) 364.
5. H. ASGEORSSON and G. GUDMUNDSSON, *Cem. Concr. Res.* **9** (1979) 249.
6. P.-C. AITCIN, P. PINSONNEAULT and G. RAU, in "Effects of Flyash Incorporation in Cement and Concrete", edited by S. Diamond (Materials Research Society, University Park, PA, 1981) p. 316.
7. L. HJORTH, in "Nordic Concrete Research", Publ. 1 (Nordic Concrete Federation, Oslo, Norway, 1982) p. 9.1; also in "Characterization and Performance Prediction of Cement and Concrete", edited by J. F. Young (The Engineering Foundation, New York, 1982) p. 165.
8. E. J. SELLEVOLD, D. H. BAGER, E. K. JENSON and T. KNUCKSEN, in "Condensed Silica Fume in Concrete", edited by O. E. Gjørv and K. J. Løland. Report BML 82.610. (Cement and Concrete Research Institute, Trondheim Institute of Technology, Trondheim, Norway, 1982) p. 19.
9. J. H. BAACHE, paper presented at 2nd International Conference on Superplasticizers in Concrete, Aalborg Portland, Aalborg, Denmark, 1981.
10. S. CHATTERJI, N. THAULOW and P. CHRISTENSEN, *Cem. Concr. Res.* **12** (1982) 781.
11. A. D. BUCK and J. P. BURKES, Proceedings of the 3rd International Conference on Cement Microscopy, Houston, TX, March, 1981 (International Cement Microscopy Association, Duncanville, TX) p. 279.
12. F. M. GRAGG and J. SKALNY, *Cem. Concr. Res.* **2** (1972) 745.
13. K. MOHAN and H. F. W. TAYLOR, in "Effects of Flyash Incorporation in Cement and Concrete", edited by S. Diamond (Materials Research Society, University Park, PA, 1981) p. 54.
14. F. D. TAMAS, A. K. SARKAR and D. M. ROY, in "Hydraulic Cement Pastes: Their Structure and Properties" (Cement and Concrete Association, Slough, UK, 1976) pp. 55.
15. J. HRILJAC, Z.-Q. WU and J. F. YOUNG, *Cem. Concr. Res.* **13** (1983) 877.
16. Z.-Q. WU and J. F. YOUNG, *J. Amer. Ceram. Soc.* **67** (1984) 48.
17. Z.-Q. WU, J. HRILJAC, C.-L. HWANG and J. F. YOUNG, *ibid.* **66** (1983) C-86.
18. I. JAWED and J. SKALNY, in "Effects of Fly-Ash Incorporation in Cement and Concrete", edited by S. Diamond (Materials Research Society, University Park, PA, 1981) p. 60.
19. S. CHATTERJI, *Cem. Concr. Res.* **10** (1980) 783.
20. A. GHOSE and P. L. PRATT, in "Effects of Flyash Incorporation in Cement and Concrete", edited by S. Diamond (Materials Research Society, University Park, PA, 1981) p. 82.
21. W. LUKAS, *Mater. Constr. (Paris)* **9** (1977) 331.
22. D. L. RAYMENT, *Cem. Concr. Res.* **12** (1982) 133.

Received 15 August
and accepted 29 November 1983